

Dynamics of a harmonic oscillator on the Bethe lattice

Jangil Kim*

*Department of Physics, College of Natural Science, Kyungpook National University, Taegu 702-701, Korea
and Department of Physics, College of Natural Science, Pusan National University, Pusan 609-735, Korea*

Isao Sawada†

Division of Materials Physics, Graduate School of Engineering Science, Osaka University, Osaka 560-8531, Japan

(Received 30 September 1999)

The velocity autocorrelation functions for a classical coupled harmonic oscillator on the Bethe lattice are exactly evaluated with use of the continued fraction formalism. A long-time tail of $t^{-3/2}$ leading to a vanishing diffusion coefficient results from the localized excitations with a gap occurring due to the nonexistence of a well-defined wave vector. The strongly colored fluctuating forces in the generalized Langevin equation are specified by the memory functions with a tail of $t^{-3/2}$.

PACS number(s): 05.60.-k, 05.20.-y, 05.40.-a, 82.20.Rp

The harmonic oscillator is a canonical model in physics of any field. The dynamical properties have been investigated, e.g., to elucidate the phenomenological study of Brownian motion and to study the transport coefficients [1–7]. This work is to show the velocity autocorrelation functions for a classical coupled harmonic oscillator on the Bethe lattice [8,9] as an ample study in higher dimensions. The time evolution on the Bethe lattice has not been studied extensively to the authors' knowledge [10]. This work also presents a many-body model where we can obtain a long-time tail of $t^{-3/2}$ for autocorrelation functions. Understanding of a long-time tail for correlation functions is one of the important problems in statistical physics [1,5–7,11–17].

The continued fraction formalism to study the dynamics of a dynamical variable A is written [18] as

$$a_0(t) = (A(t), A)(A, A)^{-1}, \quad (1)$$

$$\bar{a}_0(z) = \frac{1}{z + \frac{\Delta_1}{z + \frac{\Delta_2}{z + \dots}}} \quad (2)$$

for the Laplace transform $\bar{a}_0(z) = \int_0^\infty dt e^{-zt} a_0(t)$. The scalar product for classical systems is $(A(t), A) \equiv \langle A(t)A \rangle = Z^{-1} \int d\Gamma A(t)A e^{-\beta H}$, where $\beta = 1/k_B T$, $d\Gamma \equiv \prod_i d\mathbf{p}_i d\mathbf{q}_i$, and $Z = \int d\Gamma e^{-\beta H}$ with a canonical momentum \mathbf{p}_i and a canonical coordinate \mathbf{q}_i on a site i . The continued fraction coefficients $\{\Delta_n\}$ are written in a compact form [19,20] as

$$f_{n+1} = \sum_i \left(\frac{\partial H}{\partial p_i} \frac{\partial}{\partial q_i} - \frac{\partial H}{\partial q_i} \frac{\partial}{\partial p_i} \right) f_n + \Delta_n f_{n-1}, \quad (3)$$

$$\Delta_n = (f_n, f_n)(f_{n-1}, f_{n-1})^{-1}, \quad (4)$$

with $f_0 = A$. The boundary conditions are $\Delta_0 = 1$ and $f_{-1} = 0$. Hence the knowledge of the static quantities $\{\Delta_n\}$ is essential to understanding the dynamical behaviors of a system.

This procedure has been developed from the generalized Langevin equation [21]

$$\frac{d}{dt} A(t) = - \int_0^t ds \varphi_A(t-s) A(s) + f_A(t). \quad (5)$$

We may reformulate the memory function as

$$\varphi_A(t) = (f_A(t), f_A)(A, A)^{-1} = \Delta_1 b_1(t), \quad (6)$$

$$\bar{b}_1(z) = \frac{1}{z + \frac{\Delta_2}{z + \frac{\Delta_3}{z + \dots}}} \quad (7)$$

We also may rewrite $A(t) = \sum_{n=0} a_n(t) f_n$ and $f_A(t) = \sum_{n=1} b_n(t) f_n$ with time-dependent real functions including Eqs. (1) and (6), respectively. We note that $a_0(0) = b_1(0) = 1$. Some issues such as electron gas [22], spin systems [23–28], and strongly correlated systems [29] have been discussed using the same continued fraction formalism in quantum systems. This formalism also gives us the knowledge of dynamical equivalence [30] such as Brownian motion with two time scales [31] in different physical systems.

The Hamiltonian of a coupled harmonic oscillator reads

$$H = \frac{1}{2m} \sum_i p_i^2 + \frac{k}{2} \sum_{\langle i,j \rangle} (q_i - q_j)^2, \quad (8)$$

with a particle mass m and a force constant k . Particles interact with nearest neighbors only. Both a momentum p_i and a coordinate q_i have a single degree of freedom.

We investigate the dynamics of a momentum at a certain site on the Bethe lattice,

$$A = p_i. \quad (9)$$

Dynamics of Eq. (9) is site-independent due to the nature of the Bethe lattice. The Bethe lattice is characterized by the

*Electronic address: jikim@hyowon.pusan.ac.kr

†Electronic address: sawada@eagle.mp.es.osaka-u.ac.jp

coordination number $l \geq 2$ and becomes the pseudolattice for $l > 2$. The harmonic oscillator chain is the case with $l = 2$. A site has l first ($N = 1$) nearest neighbors and each first nearest neighbor has $l - 1$ second ($N = 2$) nearest neighbors with respect to the original site and so on. After all there are $[l(l-1)^N - 2]/(l-2)$ sites up to the N th nearest neighbors. A closed passage in the system is missing. Quite recently the Hubbard model on this lattice has been studied with the same continued fraction method [22]. Next we obtain the coefficients $\{\Delta_n\}$ by extrapolating those obtained in a finite system rigorously.

For brevity we study the dynamics of $A = p_0$ in the finite system with $l = 3$ up to the second ($N = 2$) nearest neighbors. The summation in the first term of the right-hand side of Eq. (8) thus runs over $i = 0$ to $i = 9$. The numbering of sites is as follows: 1 to 3 for the first nearest neighbors and 4 to 9 for the second ones. Using Eq. (3) and $f_0 = p_0$, we have $f_1 = -\partial H/\partial q_0 = k \sum_{i=1}^3 (q_i - q_0)$ and $(f_1, f_1) = \langle f_1^2 \rangle = 3k/\beta$. It is clear that $\Delta_1 = 3k/m$ from Eq. (4) because of $(f_0, f_0) = \langle p_0^2 \rangle = m/\beta$. The integration for the one-dimensional variables, p_i and q_i , runs over $-\infty$ through ∞ . By successive use of Eq. (3), we have $f_2 = (k/m) \sum_{i=1}^3 p_i$. Then we have $\Delta_2 = k/m$ from $(f_2, f_2) = 3(k^2/m\beta)$. Note that the factor $3 = l$ disappears at Δ_2 . We have $f_3 = (k^2/m) (\sum_{i=4}^9 q_i - 2 \sum_{i=1}^3 q_i)$, $(f_3, f_3) = 3 \times 2(k^3/m^2\beta)$, and $\Delta_3 = 2(k/m)$ with the factor $2 = l - 1$. The next basis vector is $f_4 = \sum_{i=4}^9 p_i$ and $\Delta_4 = k/m$. Since this system has finite sites, $f_5 = 0$ and thus the Hilbert space of $A = p_0$ is spanned by $\{f_{n \leq 2N}\}$ with $N = 2$. Here we must note that $\{\Delta_{n \leq 2N}\} = \{l, 1, l-1, 1\}$ in units of $k/m = 1$ with $l = 3$. If we consider a system with more sites up to, e.g., the third ($N = 3$) nearest neighbor, then we have $\{\Delta_{n \leq 2N}\} = \{l, 1, l-1, 1, l-1, 1\}$. Consequently, we may conclude that Eq. (4) is

$$\{\Delta_n\} = \{l, 1, l-1, 1, l-1, 1, l-1, \dots\} \quad (10)$$

on the Bethe lattice with $l = 3$. This is valid for arbitrary $l \geq 2$. No space for proof. The continued fraction coefficients $\{\Delta_n\}$ of Eq. (10) are not perfectly alternating because of the presence of Δ_1 , however, the spectral density obtained from those has a clear gap as shown later. The perfectly alternating $\{\Delta_n\}$ have been shown in Ref. [25], but the corresponding models have not been specified there. Such $\{\Delta_n\}$ have not been obtained so far except the Bethe lattice [29], but may be obtainable in a system with a gap [16].

We rewrite the function $F(t) = (2\pi i)^{-1} \int dz e^{zt} \bar{F}(z)$ such as Eqs. (1) and (6) to introduce the spectral density $\text{Re } \bar{F}(-i\omega^+)$ as

$$F(t) = \frac{1}{\pi} \int_{-\infty}^{\infty} d\omega \cos \omega t \text{Re } \bar{F}(-i\omega^+), \quad (11)$$

with $\omega^+ = \omega + i0^+$. We substitute Eq. (10) for $\{\Delta_{n \geq 1}\}$ in Eq. (2) and $\{\Delta_{n \geq 2}\}$ in Eq. (7) to have, respectively,

$$\bar{a}_0(z) = \frac{(2-l)(z^2+l) + l\sqrt{(z^2+a^2)(z^2+b^2)}}{2z(z^2+c^2)}, \quad (12)$$

$$\bar{b}_1(z) = \frac{l-2-z^2 + \sqrt{(z^2+a^2)(z^2+b^2)}}{2(l-1)z}, \quad (13)$$

with $a = \sqrt{l-1} - 1$, $b = \sqrt{l-1} + 1$, and $c = \sqrt{2l}$ in units of the characteristic frequency $\sqrt{k/m} = 1$. Equations (12) and (13) hold the relation $z\bar{a}_0(z) - 1 = -\Delta_1 \bar{b}_1(z)\bar{a}_0(z)$, which is obtained through taking the inner product of Eq. (9) and both sides of Eq. (5).

The diffusion coefficient defined by $D = \int_0^\infty dt \langle v_i(t)v_i \rangle = (m\beta)^{-1} \int_0^\infty dt a_0(t)$ with $v_i = p_i/m$ is rewritten as

$$D = \lim_{t \rightarrow \infty} D(t) = \frac{1}{m\beta} \text{Re } \bar{a}_0(-i0^+), \quad (14)$$

$$D(t) = \frac{1}{\pi m\beta} \int_{-\infty}^{\infty} d\omega \frac{\sin \omega t}{\omega} \text{Re } \bar{a}_0(-i\omega^+). \quad (15)$$

For the coordination number $l = 2$, the system becomes a harmonic oscillator chain and includes no features of the Bethe lattice. Equation (10) reproduces the results $\{\Delta_n\} = \{2, 1, 1, 1, \dots\}$ obtained in Ref. [30]. Equations (12) and (13) become $a_0(z) = 1/\sqrt{z^2+4}$ and $b_1(z) = (\sqrt{z^2+4}-z)/2$, respectively. We then have Eqs. (1), (6), and (14) as

$$\frac{\langle p_i(t)p_i \rangle}{\langle p_i^2 \rangle} = J_0(2t), \quad (16)$$

$$\varphi_{p_i}(t) = \frac{2J_1(2t)}{t}, \quad (17)$$

$$D = \frac{1}{2m\beta}, \quad (18)$$

where $J_{0(1)}$ is the Bessel function of the order of 0(1). Equation (16) has a tail of $t^{-1/2}$, but Eq. (15) with $t = \infty$ converges to Eq. (18). This is identical to Eq. (14) with $\text{Re } \bar{a}_0(-i0^+) = 1/2$. Equation (17) has a tail of $t^{-3/2}$. We have $\int_0^\infty dt \varphi_{p_i}(t) = 2 \text{Re } \bar{b}_1(-i0^+) = 2$. The finite values together with Eq. (18) are inconsistent with the fact that the particle is fixed up at a site with vibration on a uniform chain [5]. This inconsistency is due to the existence of acoustic mode in the system with the boundary condition in the thermodynamic limit [6]. Furthermore the dynamical variable given by Eq. (9) does not show Brownian motion because there is a single time scale in both Eqs. (16) and (17). Equation (14) in this system has no meaning of diffusion coefficient.

For the coordination number $l \geq 3$, the characteristic features of the Bethe lattice have appeared explicitly. Using Eq. (12) the spectral density of Eq. (1) is

$$\text{Re } \bar{a}_0(-i\omega^+) = \frac{\sqrt{b^2 - \omega^2} \sqrt{1 - (a/\omega)^2}}{4} \Theta(\omega), \quad (19)$$

where $\Theta(\omega) = \theta(|\omega| - a)\theta(b - |\omega|)$ with a step function. Equation (19) is determined by the conditions for the relevant part of the spectral density [30] and corresponds to the branch cuts in evaluation of the inverse Laplace transform. The contribution from the isolated pole vanishes. Equation (19) is identical to the spectra obtained by the phonon Green's function [8,9]. The Bethe lattice with $l \geq 3$ has a gap in the spectral density. This feature must be compared to the case with $l = 2$ as shown before. The reason why a gap opens

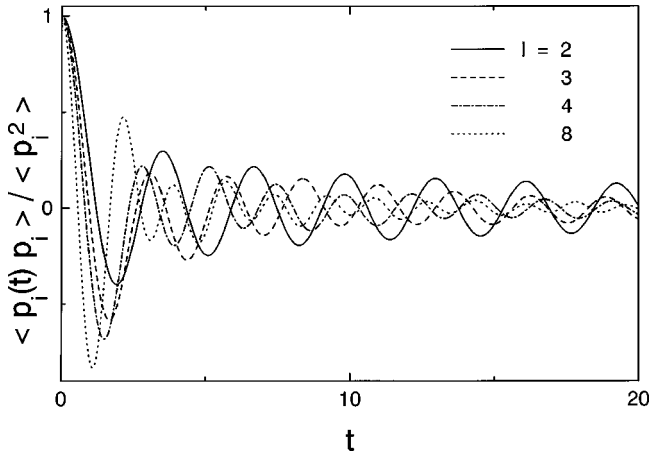


FIG. 1. Velocity autocorrelation functions for a few l 's together with Eq. (16). A long-time tail for $l \geq 3$ is $t^{-3/2}$ when we plot them in a log-log scale not shown here. A tail of $t^{-1/2}$ for $l=2$. The frequency unit is $\sqrt{k/m}$ with a force constant k and a particle mass m .

in the spectral density would be related to the missing of the acoustic lattice vibration due to the structure of pseudolattice with this case. The wave number cannot be defined conventionally and the localized excitation would take place. A similar gap in the one-particle density of states has been reported in the Hubbard model on the Bethe lattice [29].

Noting $0 < a < b < c$ we can expand the factor in Eq. (19) as

$$\sqrt{1 - (a/\omega)^2} / [1 - (\omega/c)^2] = \sum_{k=0}^{\infty} [g_k(l)\omega^{-2k} + h_k(l)\omega^{2k}],$$

with

$$g_k(l) = - \sum_{j=k}^{\infty} A_j a^{2j} c^{2(k-j)},$$

$$h_k(l) = - \sum_{j=k}^{\infty} A_{j-k} a^{2(j-k)} c^{-2j},$$

$$A_j = (2j-1)!! / [2^j (2j-1)j!],$$

and $A_0 = -1$. Furthermore, putting $\omega = b \sin \theta$ and using an identity, $\cos(bt \sin \theta) = \sum_{n=-\infty}^{\infty} \cos 2n\theta J_{2n}(bt)$, we obtain the velocity autocorrelation function of Eq. (1) with the Bessel function of the order of even integer as

$$a_0(t) = \frac{\langle p_i(t)p_i \rangle}{\langle p_i^2 \rangle} = \sum_{n=-\infty}^{\infty} [G_n(l) + H_n(l)] J_{2n}(bt),$$

$$G_n(l) = \sum_{k=0}^{\infty} \frac{g_k(l)}{b^{2k-2}} \frac{1}{2\pi} \int_{\alpha}^{\pi/2} d\theta \frac{(\cos \theta)^2}{(\sin \theta)^{2k}} \cos(2n\theta),$$
(20)

$$H_n(l) = \sum_{k=0}^{\infty} \frac{h_k(l)}{b^{-2k-2}} \frac{1}{2\pi} \int_{\alpha}^{\pi/2} d\theta \frac{(\cos \theta)^2}{(\sin \theta)^{-2k}} \cos(2n\theta),$$

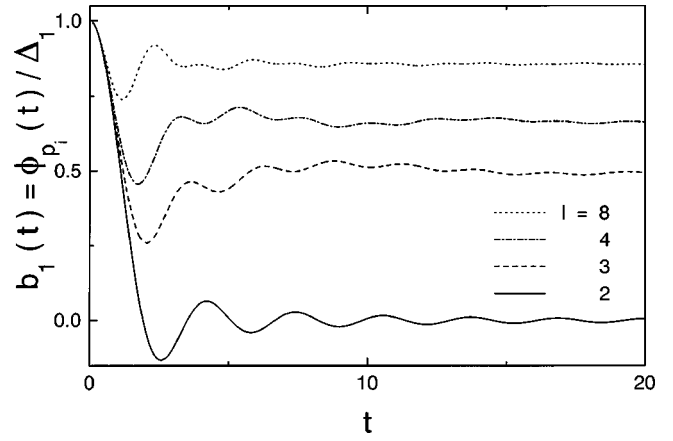


FIG. 2. Memory functions scaled by $\Delta_1=l$ for a few l 's together with Eq. (17). Short time expansion gives $b_1(t) = 1 - t^2/2$ irrespective of l . A tail of $t^{-3/2}$ is observed in $b_1(t) - b_1(t=\infty)$ when we plot them in a log-log scale.

with $\alpha = \arcsin(a/b)$. Temperature dependence in Eq. (20) disappears due to the normalization by $\langle p_i^2 \rangle = m/\beta$.

Similarly we have the spectral density of Eq. (6) from Eq. (13) as

$$\text{Re } \bar{b}_1(-i\omega^+) = \frac{l-2}{l-1} \pi \delta(\omega) + \frac{\sqrt{(b^2 - \omega^2)[1 - (a/\omega)^2]}}{2(l-1)} \Theta(\omega).$$
(21)

Unlike Eq. (19) there is a term with $\delta(\omega)$ in Eq. (21) contributed from a pole at $z=0$ in evaluation of Eq. (11). This is because the alternation in $\{\Delta_{n \geq 2}\}$ for Eq. (7) is inverse to that in $\{\Delta_{n \geq 1}\}$ for Eq. (2) [25]. We thus obtain Eq. (6) in the similar way to Eq. (20) as

$$\varphi_{p_i}(t) = \frac{l}{l-1} \left[l-2 + \sum_{n=-\infty}^{\infty} I_n(l) J_{2n}(bt) \right],$$
(22)

$$I_n(l) = \sum_{k=0}^{\infty} \frac{A_k}{b^{2k-2}} \frac{1}{\pi} \int_{\alpha}^{\pi/2} d\theta \frac{(\cos \theta)^2}{(\sin \theta)^{2k}} \cos(2n\theta).$$

To illustrate the time evolutions of interest, we show the numerical calculations of Eqs. (1), (6), and (15) with use of Eqs. (11), (19), and (21) in Figs. 1, 2, and 3, respectively. The characteristic time scale t_0 defined by the first zero point such that $a_0(t_0) = 0$ is roughly equal to $\sqrt{2/l}$. For $t \leq t_0$, we have $\langle p_i(t)p_i \rangle / \langle p_i^2 \rangle = 1 - t^2/2$, $b_1(t) = 1 - t^2/2$, and $D(t)m\beta = t$ to be observed in Figs. 1, 2, and 3, respectively.

For $t \geq t_0$, a glance at the analytical expressions in Eqs. (20) and (22) brings us a misleading tail of $t^{-1/2}$. A tail observed in Figs. 1 and 2 is in fact $t^{-3/2}$, which holds true for arbitrary $l \geq 3$, is originated from the structure of the spectral density. To see this mathematically we go back to Eq. (11) with Eq. (19). After performing the partial integration we have

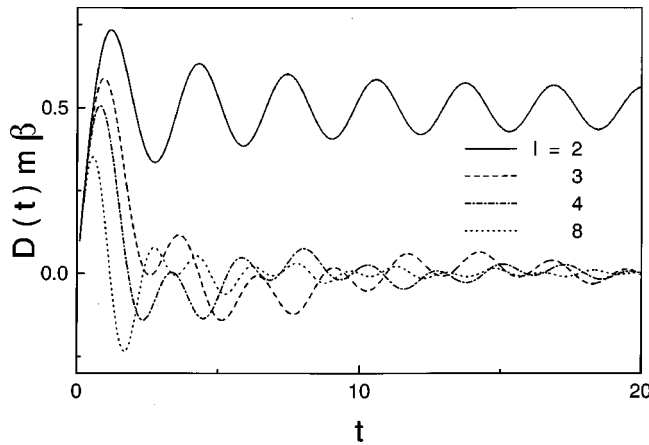


FIG. 3. Time-dependent diffusion coefficients for a few l 's together with the case for $l=2$. A time tail of them is the same as in the velocity autocorrelation functions, i.e., $t^{-3/2}$ for $l \geq 3$ and $t^{-1/2}$ for $l=2$. The vanishing convergent value is identical to Eq. (14) with $\text{Re } \bar{a}_0(-i0^+) = 0$.

$$a_0(t) = -\frac{2}{\pi t} \int_a^b d\omega \sin \omega t \frac{d}{d\omega} \text{Re } \bar{a}_0(-i\omega^+). \quad (23)$$

Since the first derivative in the vicinity of the boundaries diverges as $(b-\omega)^{-1/2}$ and $(\omega-a)^{-1/2}$, the integration in Eq. (23) would behave like the Bessel function as shown in Eq. (16). Thus, a tail of $t^{-3/2}$ for Eq. (20) is verified. Similar consideration is given to a tail in Eq. (22). This tail reminds us of higher dimension studies such as those in Refs. [1,11]. If the first derivative converges, then we have a tail of t^{-1} as obtained in Refs. [16,17], where the relaxation functions and the memory functions for the current operator in the two-band Bloch electrons have calculated.

The conventional Brownian motion with white noise is described by the frequency-independent spectral density and lead to the memory function of Eq. (6) written with $\delta(\omega)$. On the contrary, this system shows the strongly colored spectral density. The strongly colored factor meant by $\Theta(\omega)$ guarantees the existence of a tail. The structure of the spectral density determines the power of a tail. Therefore, we need physical grounds for such a structure; however, no solid candidates except the localized excitation can be allowed for this system. This is because there exists no well-defined wave vector. The quantal case is expected to have a tail for Eqs. (1) and (6) due to a similar reason. A tail of t^{-1} in Refs. [16,17] originates from the spontaneous strongly colored quantum fluctuations.

If an impurity sits on the site $i=0$, then we must replace $(\lambda/2m)p_0^2 + (\alpha k/2)\sum_{j=1}^l (q_0 - q_j)^2$ for the corresponding term in the Hamiltonian Eq. (8). The mass m_0 and the force constant k_0 is written as $\lambda = m/m_0$ and $\alpha = k_0/k$, respectively. The autocorrelation function of $A=p_0$ is determined by $\{\Delta_n\} = \{l\lambda\alpha, \alpha, l-1, 1, l-1, 1, l-1, \dots\}$. The detailed study will be published sometime in the future [32].

To summarize, we have investigated the dynamics of a classical coupled harmonic oscillator on the Bethe lattice to obtain the velocity autocorrelation functions with a tail of $t^{-3/2}$ leading to a vanishing diffusion coefficient. This tail results from the localized excitations with a gap in the spectral density due to the nonexistence of a well-defined wave vector. The strongly colored fluctuating forces $f_A(t)$ in Eq. (5) are specified by the memory functions with a tail of $t^{-3/2}$.

The authors are grateful to the hospitality of KIAS, Seoul, Korea, where a portion of this work was done. They thank Jaesuk Kim for his assistance. J. K. appreciates the support by Korea Research Foundation (Grant No. 1998-001-D00305) and by the PD program of Kyungpook National University, 1999. I. S. is supported by the Japan Society for the Promotion of Science.

-
- [1] P. Mazur and E. Montroll, *J. Math. Phys.* **1**, 70 (1960).
[2] R.J. Rubin, *J. Math. Phys.* **1**, 309 (1960).
[3] G.W. Ford, M. Kac, and P. Mazur, *J. Math. Phys.* **6**, 504 (1965).
[4] K. Wada and J. Hori, *Prog. Theor. Phys.* **49**, 129 (1973).
[5] R.F. Fox, *Phys. Rev. A* **26**, 3216 (1983).
[6] J. Florencio, Jr. and M.H. Lee, *Phys. Rev. A* **31**, 3231 (1985).
[7] H.K. McDowell and A.M. Clogston, *J. Stat. Phys.* **67**, 331 (1992).
[8] K. Wada, T. Fujita, and T. Asahi, *Prog. Theor. Phys.* **59**, 1101 (1978).
[9] T. Tsuchiya, *Prog. Theor. Phys.* **60**, 1249 (1978).
[10] V.E. Zdobov and M.A. Popov, *Theor. Math. Phys.* **112**, 1182 (1997).
[11] B.J. Alder and T.E. Wainwright, *Phys. Rev. A* **1**, 18 (1970).
[12] H. van Beijeren, *Rev. Mod. Phys.* **54**, 195 (1982).
[13] F. den Hollander, J. Naudts, and P. Scheunders, *J. Stat. Phys.* **66**, 1527 (1992).
[14] F. den Hollander, J. Naudts, and F. Redig, *J. Stat. Phys.* **69**, 731 (1992).
[15] R. Brito, G.A. van Velzen, F. den Hollander, J. Naudts, and F. Redig, *J. Stat. Phys.* **80**, 565 (1995).
[16] I. Sawada, *J. Phys. Soc. Jpn.* **65**, 3100 (1996).
[17] I. Sawada, *Progress in Statistical Physics*, edited by W. Sung *et al.* (World Scientific, Singapore, 1998), p. 342.
[18] H. Mori, *Prog. Theor. Phys.* **34**, 399 (1965).
[19] M.H. Lee, *Phys. Rev. B* **26**, 2547 (1982).
[20] M.H. Lee, *Phys. Rev. Lett.* **49**, 1072 (1982).
[21] H. Mori, *Prog. Theor. Phys.* **33**, 423 (1965).
[22] J. Hong and M.H. Lee, *Phys. Rev. Lett.* **70**, 1972 (1993).
[23] M.H. Lee, I.M. Kim, and R. Dekeyser, *Phys. Rev. Lett.* **52**, 1579 (1984).
[24] J. Florencio, Jr. and M.H. Lee, *Phys. Rev. B* **35**, 1835 (1987).
[25] V.S. Viswanath and G. Müller, *The Recursion Method* (Springer, Berlin, 1994).
[26] V.S. Viswanath, S. Zhang, G. Müller, and J. Stolze, *Phys. Rev. B* **51**, 368 (1995).
[27] S. Sen and T.D. Blerssch, *Physica A* **253**, 178 (1998).
[28] I. Sawada, *Phys. Rev. Lett.* **83**, 1668 (1999).
[29] J. Hong and H.-Y. Kee, *Phys. Rev. B* **52**, 2415 (1995).
[30] M.H. Lee, J. Florencio, Jr., and J. Hong, *J. Phys. A* **22**, L331 (1989).
[31] S. Sen, *Phys. Rev. B* **53**, 5104 (1996).
[32] J. Kim and I. Sawada (unpublished).